

Molten shell-activated, high-performance, un-doped Li_4SiO_4 for high-temperature CO_2 capture at low CO_2 concentrations

Ke Wang^{1,2}, Feng Gu¹, Peter T. Clough², Youwei Zhao¹, Pengfei Zhao¹, Edward J. Anthony^{2*}

¹ School of Electrical and Power Engineering, China University of Mining and Technology, Xuzhou 221116, China.

² Energy and Power Theme, Cranfield University, Cranfield, Bedfordshire, MK43 0AL, UK.

Ke Wang is currently visiting Cranfield University.

* Corresponding author: Edward J. Anthony, E: b.j.anthony@cranfield.ac.uk, T: +44 (0) 1234 752 823

Abstract: Lithium orthosilicate (Li_4SiO_4) represents a potential class of high-temperature sorbents for CO_2 capture in power plants and sorption enhanced methane reforming to produce H_2 . However, conventional wisdom suggests that pure Li_4SiO_4 would have extremely slow sorption kinetics at realistic low CO_2 concentrations. Here, we report the opposite result: using a simple and cost-effective glucose-based mild combustion procedure, an unusually efficient and pure form of Li_4SiO_4 (MC-0.6) was synthesized to achieve a maximum uptake capacity of 35.0 wt.% at 580 °C for CO_2 concentrations under 15 vol.% and maintained this capacity over multiple cycles. The characterization results showed that highly porous nano-agglomerate-like (50-100 nm) morphologies were apparent and ensured a rapid surface-sorption of CO_2 . In this process, a macroporous nano-sized Li_2SiO_3 cover on the melt layer of Li_2CO_3 was

identified for the first time. This special structure appeared to accelerate the transportation of CO₂ and the diffusion of Li⁺ and O²⁻ through a molten layer enhancing contact with CO₂. Thus, the sample MC-0.6 reduced both the surface-sorption and diffusion kinetics dependence on low CO₂ concentrations. Rather than use traditional approaches (controlled morphologies combined with doping), we have demonstrated that the slow kinetics can be overcome simply by a controlled morphologies strategy, which opens up a new direction for the synthesis of high-performance Li₄SiO₄ sorbents.

Keywords: CO₂ capture; Li₄SiO₄; power plants

1. Introduction

Excessive anthropogenic CO₂ emissions have been led to dangerous climate breakdown [1]. Fully decarbonizing global industry and society are essential to limit global warming to 2 °C, which was the commitment agreed at the 21st Conference of Parties [2]. To achieve such an ambitious target, key supply-side technologies include novel energy-storage systems, carbon capture and utilization (CCUS) and zero-carbon electricity production are proposed [3]. Among these, CCUS using various high-temperature solid sorbents (hydrotalcites [4], MgO-based sorbents [5, 6], ceramic materials [7], and calcium oxides [8-10]), have been considered as promising approaches for mitigating CO₂ emissions from the top-emitting industries, namely: power plants, cement, iron & steel, and chemicals & plastics owing to their potential for increased useful energy production and decreased operating costs [11]. Moreover, these high-temperature sorbents are suitable for sorption enhanced methane reforming processes by shifting the thermodynamic equilibrium towards the production of high

H₂ yields, such as in the Sorption Enhanced Steam Methane Reforming (SESMR), the Sorption Enhanced Chemical Looping Reforming of Methane (SE-CL-RM), and the Super-Dry Chemical Looping Reforming of Methane (SD-CL-RM) [12-14]. Among suitable materials for such processes, alkaline ceramic materials [7] (Li₂ZrO₃, Li₂CuO₂, Li₅AlO₄, Na₂ZrO₃ and so on), in particular lithium orthosilicate (Li₄SiO₄), has been recognized as one of most promising potential candidates because of its large theoretical capacity (36.7 wt.%), reasonable costs, and more importantly greater cyclic stability and lower regeneration temperature as compared with other high-temperature sorbents [15].

Since Kato and Nakagawa [16] first reported the use of Li₄SiO₄ sorbents in 2001, various preparation methods such as solid-state [17], hydration [18], sol-gel [19], carbon templates [20], impregnated precipitation [21], ball milling [22], solvo-plasma [23] and combustion [24] have been used to control the morphologies (and typically work by reducing particle size or improving pore structure porosity) of Li₄SiO₄ sorbents. Utilization of more appropriate silicon or lithium sources were also suggested to improve the porosity [25, 26]. Unfortunately, while these structurally improved Li₄SiO₄ sorbents demonstrated higher carbonation conversion (>90%) in pure CO₂ at 700 °C, such concentrations are far from realistic conditions. Thus, under typical sorption enhanced methane reforming conditions, concentrations are typically around 4-15 vol.% CO₂, and the carbonation needs to occur at relatively lower temperatures (400~600 °C). Also, as carbonation progresses, a dense and solid product layer covers the unreacted core of Li₄SiO₄ [27], producing poor sorption kinetics [28]. Thus, a low conversion

frequently occurs within a given residence time.

To further enhance the sorption kinetics in a diluted CO₂ atmosphere, the approach for achieving control morphologies combined with doping was developed. Doping Li₄SiO₄ with various types of foreign materials [29-33], in particular eutectic alkali salts [34, 35], have been shown to be favorable for reducing the diffusion resistance through the formation of low-temperature molten shell. For these doped sorbents, their sorption kinetics were not only dependent on the morphologies of the Li₄SiO₄ precursor but also related to the types of dopants [15]. These alkali dopants can be classified into three categories, i.e., single component, double salts, and multiple salts. The most popular single dopant was alkali metal carbonates, such as potassium carbonate (K₂CO₃) [36] or sodium carbonate (Na₂CO₃) [37]. Our group [38, 39] has further developed several types of sodium halides as new dopants. Beside the formation of different eutectic phases, these sodium halides doped Li₄SiO₄ samples also improved the CO₂ superficial chemisorption kinetics, due to the generation of a Li₂O enriched surface. For double salts, e.g. K₂CO₃ and Na₂CO₃ co-doped Li₄SiO₄ demonstrated higher capacities in diluted CO₂ atmosphere due to the formation of molten potassium-sodium double carbonates [34, 37]. Considering the lower melting temperature of Li₂CO₃, multiple salts such as (Li-Na-K)CO₃ have also been introduced [40]. Although doped Li₄SiO₄ demonstrate improved kinetics at low CO₂ partial pressure, three major limitations need to be eliminated: I) The amount of inert dopant was relatively high in most doped Li₄SiO₄ (in some cases was up to 30 wt.%), greatly reducing the theoretical capacity on a mass basis [34]. II) Their cyclic durability was

decreased due to the grain aggregation and porosity loss generated by eutectic alkali salts [34, 37]. III) The presence of eutectic alkali salts can cause severe catalyst sintering in the sorption enhanced reforming process, in turn leading to serious decreases in H₂ production [15]. However, these limitations can be eliminated if a suitable non-doped Li₄SiO₄ can be developed. However, conventional wisdom [7] implicit in all these studies suggests pure Li₄SiO₄ has poor kinetics under diluted CO₂ atmosphere, highlighting the fact that synthesizing pure Li₄SiO₄ with simultaneously large increases in kinetics and durability remains largely unexplored.

Here, we challenge this conventional wisdom by developing a highly efficient pure Li₄SiO₄ sorbent, suitable for CO₂ capture at a low CO₂ concentration of 15%, via a simple and cost-effective glucose-based mild combustion procedure. Further, a detailed understanding of the intrinsic properties of Li₄SiO₄ were explored by examining their crystal phases, morphologies, pore structures, surface compositions, melting behavior and CO₂ sorption kinetics. For the first time, the existence of eutectic behavior on non-doped Li₄SiO₄ with the sorption CO₂ is confirmed. A new CO₂ sorption mechanism, termed here “nanoporous morphologies induced molten shell” is highlighted given its remarkably improved capture performance.

2. Experimental

2.1 Sorbents

All chemicals used were analytical grade (from the Aladdin Chemical Reagent Co., Ltd.). The Li₄SiO₄-based sorbents were synthesized via a mild combustion procedure using LiNO₃, glucose and fumed silica as the oxidizer, fuel and Si precursors were used.

In a typical synthesis, LiNO_3 , glucose and fumed silica with a molar ratio of 68:44:17 were first dissolved in 100 mL of deionized water under vigorous stirring in a water bath at 80 °C, with heating continuing until the solution was completely evaporated. Then, the resulting dry gel was pyrolyzed at 500 °C in pure N_2 and finally calcined at 700 °C for 4 h in air. In these experiments, the glucose: LiNO_3 molar ratio was varied from 0.4:1 to 0.8:1 during the mild combustion process. Here, the baseline sorbent obtained from mild combustion was designated as MC-0.6, where the number represents the molar ratio of glucose: LiNO_3 . For comparison, two Li_4SiO_4 sorbents were also prepared using normal combustion (without the pyrolysis step) and a solid-state method (the absence of glucose), which were named CC and SS, respectively.

2.2 Characterization

The phase composition of the samples was identified by an X-ray diffractometer (XRD, Bruker Model D8 Advance) in the 2θ range of 10-70°. A Hitachi Model S-4800 scanning electron microscope (SEM) was used to analyze the morphologies of the samples. The textural properties, including the specific surface area, pore volume and size distribution were obtained using a Quantachrome Novawin N_2 adsorption/desorption analyzer. X-ray photoelectron spectroscopy (XPS) spectra were obtained using a Perkin-Elmer PHI 5600 XPS to analyze the surface atomic concentrations and bonding. The differential scanning calorimetry (DSC) data were obtained with a Labsys Evo simultaneous thermal thermogravimetric analyzer under 15 vol.% CO_2 , from 100 °C to 800 °C, with a heating rate of 10 °C/min and a flow rate of 0.05 dm^3/min .

2.3 CO₂ capture performance

The CO₂ capture performance was measured using a thermogravimetric analyzer (ZRY-1P, Techcomp Jingke Scientific Instrument Co., Ltd., Shanghai, China). The samples were weighed, placed in an alumina crucible, and heated from room temperature to 900 °C at a heating rate of 10 °C/min under a 15 vol.% CO₂ atmosphere balanced with N₂ with a total flow rate of 0.05 dm³/min. Using the same gas flow, isothermal sorption experiments were carried out at 200, 500, 540, 580 and 600 °C for 120 min. The desorption of the sorbents included the following steps: in a pure CO₂ atmosphere, the sample was heated to 700 °C for 120 min to approaching the saturated sorption; the atmosphere was immediately switched to pure N₂ and maintained at this temperature for desorption. The cyclic sorption and desorption of MC-0.6 for 10 cycles was also studied, in which the sorption step lasted for 20 min at 580 °C with a flow of 15% CO₂ in N₂ and desorption was performed at 700 °C in pure N₂ for 5 min.

3. Results and discussion

3.1 CO₂ uptake characteristics

The CO₂ uptake performances of three samples derived from solid-state, common combustion and mild combustion were compared. Here, the dynamic sorption under 15 vol.% CO₂ from 100 °C to 900 °C is shown in Fig. 1a. The reference SS only presents a one-step sorption process with a slow sorption occurring at ~500 °C due to a slight weight increase and attained a maximum weight increment of only 10.1 wt.% at ~620 °C. This poor sorption performance of pure Li₄SiO₄ has also been seen in previous studies [41, 42]. However, above 620 °C the weight increment gradually decreased

since desorption was activated. Different from the case of SS, a similar three-step sorption process was observed for CC and MC-0.6. Initially, a small weight increment of 2.5 wt.% was seen for both samples between 100 and ~400 °C, where a slow superficial-sorption occurred. Ball milled treated Li_4SiO_4 has also previously been reported to demonstrate only low capture CO_2 at such low temperatures [43]. However, a second sudden and rapid weight increment followed, where a fast-sorption began. Finally, between 550 and ~620 °C, the sorption rates became relatively sluggish where a third slow-diffusion step took place. Moreover, compared with CC, MC-0.6 presented higher sorption rates for the second and third steps. Thus, a higher maximum CO_2 sorption of 32.5 wt.% was achieved for MC-0.6 than the case of CC (26.9 wt.%).

Isothermal tests at 580 °C under 15 vol.% CO_2 are evaluated in Fig. 1b. During the 120 min sorption process, the SS exhibited too slow a weight increment to allow one to distinguish the transition between a rapid sorption step and a slow diffusion step. Thus, its sorption was not saturated even after 120 min although it demonstrated a significantly small final CO_2 uptake of 13.0 wt.%. By comparison, a noticeably faster sorption with a higher weight increase of 25.1 wt.% was recorded in the first 10 min of the CC's isotherm. Subsequently, a slow diffusion carbonation rate, with a gradual weight increase, was observed and the final CO_2 uptake exceeds 27.5 wt.%. Similar, but even more dramatic behavior was observed for the isotherm of MC-0.6. Here sorption quickly reached a level of 32.5 wt.% within 10 min and a larger maximal sorption capacity of 35.0 wt.% after 120 min (corresponding to 95% conversion), which is the highest value for pure Li_4SiO_4 under 15 vol.% CO_2 reported in the literature to

date. This excellent CO₂ sorption demonstrates that the poor CO₂ sorption kinetics of pure Li₄SiO₄ at a low CO₂ concentration can be overcome by controlling microstructural properties using the mild combustion procedure employed here rather than using eutectic dopants. In addition, the optimal amount of glucose (glucose: LiNO₃ molar ratio) was determined to be 0.6, as shown in Fig. 1c.

To further analyze the CO₂ capture process of MC-0.6, isothermal tests were evaluated at 200, 500, 540, 580 and 600 °C for 120 min. As shown in Fig. 1d, a low sorption rate and capacity was obtained at 200 °C, agreeing well with dynamic sorption results (Fig. 1a) and confirming that slow superficial-sorption can occur even at such a low temperature. When the temperature was increased to 500 °C, a fast-sorption was observed with a slightly enhanced CO₂ uptake. When the temperature was further increased to 540 °C, an even faster sorption rate and higher CO₂ sorption capacity was attained. At an even higher temperature (580 °C), this sorption achieved its highest reaction rate and largest capacity. However, beyond this, at 600 °C, the desorption process starts to dominate and this results in a decreased sorption rate and capacity. Apparently, over a relatively wide range of temperatures (540-580 °C), the maximum sorption capacity of MC-0.6 exceeds 25 wt.%. Fast kinetics and large capacity at a relatively wide range of temperatures are particularly desirable for sorption enhanced reforming conversions of methane process since the *in-situ* CO₂ removal should be rapid and high enough to yield high purity H₂ [12].

The cyclic performance of MC-0.6 was examined through 10 sorption/desorption cycles. As shown in Fig. 1e, the initial CO₂ uptake of MC-0.6 reached 32.5 wt.% upon

sorption at 580 °C for 20 min. After 10 cycles, its uptake still maintained levels of 30.0 wt.%, confirming the stable regeneration performance. To explore its excellent regeneration properties, the decomposition behavior of MC-0.6 and SS were studied. As shown in Fig. 1f, nearly 95% of the CO₂ was released after 5 min at 700 °C for MC-0.6 whereas double the time was needed for SS, suggesting that MC-0.6 demonstrates better CO₂ desorption properties, and in turn will be more energy efficient for practical applications. In this context, it should be noted, that the Na-doped Li₄SiO₄ system is reported to suffer from incomplete regeneration even at a high temperature (800 °C) [37]. Here, it is evident that because of the shorter decomposition time, which reduced the sintering of the cycled MC-0.6, it is able to demonstrate good cyclic performance.

3.2 Kinetic analysis

The sorption kinetics of CO₂ on SS, CC and MC-0.6 performed at 580 °C, were fitted to a double exponential model [17]:

$$y=A\exp^{-k_1t} + B\exp^{-k_2t} + C \quad (1)$$

Where y represents the CO₂ sorption capacity; t is the time; A , B and C are the pre-exponential factors; and k_1 and k_2 are the exponential constants indicating CO₂ surface-sorption rate and the CO₂ sorption controlled by diffusion processes, respectively.

Their sorption behavior is well described by the double exponential model. The estimated parameter values are presented in Table 1. For three sorbents, all the values of k_1 were one order of magnitude larger than those of k_2 , suggesting that the diffusion process is the rate-limiting step for the entire CO₂ sorption. Furthermore, both the k_1 and k_2 values for MC-0.6 are among the highest, convincingly demonstrating that the

mild combustion route greatly enhanced the CO₂ sorption kinetics.

To further analyze the influence of temperature on the sorption kinetics of MC-0.6, different isothermal experiments at 500, 540 and 580 °C were all fitted well by the double exponential model. As expected, both k_1 and k_2 for MC-0.6 (Table 1) increased with increasing temperature. Using Eyring's model (equation 2), the temperature dependence of the sorption kinetics can then be explored. Here, plots of $\ln(k/T)$ versus $1/T$ show linear trends, allowing their activation enthalpies to be estimated:

$$\ln(k/T) = (-\Delta H^{++}/R) 1/T + \ln(k_B/h) + \Delta S^{++}/R \quad (2)$$

where k stands for the reaction rate constant, T is the absolute temperature, ΔH^{++} is the activation enthalpy, R is the gas constant, k_B is the Boltzmann constant, h is Planck's constant and ΔS^{++} is the activation entropy.

As shown in Fig. 2, the ΔH^{++} values for the surface sorption process obtained were 18.7 kJ/mol for MC-0.6. This value is remarkably smaller than the case of other pure Li₄SiO₄ sorbents using different preparation methods [44, 45], implying that surface sorption for MC-0.6 is less reliant on temperature. While for the bulk diffusion period, the ΔH^{++} of MC-0.6 was 54.0 kJ/mol, which is smaller than the case of other pure Li₄SiO₄ sorbents as previously reported [44, 45]. Apparently, MC-0.6 has lower activation enthalpies for both the surface-sorption and diffusion processes, mainly attributed by its large specific surface area and small particle/crystal size, which will be confirmed by the following characterization results.

3.3 Characterization

To explain the superior sorption performance, the crystal phases, morphologies,

pore structures, surface compositions and melting behaviors were investigated by XRD, SEM, nitrogen adsorption, XPS and DSC. The XRD patterns (Fig. 3a) showed the standard diffraction peaks of Li_4SiO_4 , as for all three samples. No impurity phases (Li_2SiO_3 or Li_2CO_3) were identified, confirming that the preparation produced pure Li_4SiO_4 . Furthermore, according to the intensities derived from three samples, the crystallite size was ranked as follows: SS > CC > MC-0.6. During the solid-state method, the crystallite size of Li_4SiO_4 readily grows and aggregates. With the help of combustion between oxidizer (LiNO_3) and fuel (glucose), the crystal growth was greatly inhibited. Moreover, prior to the formation of Li_4SiO_4 during mild combustion step, the occurrence of the pyrolysis process under a N_2 atmosphere not only slowly removed molecules that would later add “combustion” heat but also generates carbonaceous intermediates, which serve as a dispersant and greatly suppressed crystallite growth; thus, the smallest crystallite size was obtained in MC-0.6.

The morphologies were examined using SEM, as illustrated in Fig. 4a. The SS was composed of large and dense aggregate ($\sim 10\ \mu\text{m}$) with a smooth and nonporous surface (Fig. 4a). This markedly sintered morphology can prevent CO_2 diffusion. By contrast, CC-0.6 appeared as a wormhole-like structure (Fig. 4b) consisting of a slightly intertwined pore framework (insert pictures), likely facilitating CO_2 sorption. Comparatively, the surface of MC-0.6 became looser and more fragile (Fig. 4c) and formed a sponge-like architecture. The insert further showed agglomerates of small nanoparticles (50-100 nm) combined with the presence of evident macropores.

The porous structures were examined using isothermal N_2 adsorption-desorption.

Based on the IUPAC classifications, the isotherm for SS (Fig. 5a) was type II with a narrow H3 hysteresis, corresponding to a nonporous feature. This structure agrees well with the characteristics of the sample produced in the solid-state reaction. As shown in Table 2, the SS presented a significantly smaller specific surface area ($0.4 \text{ m}^2/\text{g}$) and pore volume, agreeing with the sintered morphology as illustrated in the SEM images. Compared to SS, both CC and MC-0.6 obtained a more porous structure while their isotherm was not significantly changed. The large amount of gas released during combustion contributed to greater specific surface area (Table 2) and wormhole-like structure (Fig. 4b) in CC. Furthermore, burning of the carbonaceous intermediates can induce additional pore volume. The pore size distribution (Fig. 5b) curves also provided evidence that MC-0.4 presented the large number of macropores ($>50\text{nm}$). As a result, the largest specific surface area ($17.4 \text{ m}^2/\text{g}$) were achieved for MC-0.6.”

Compared with the case of SS, the above XRD, SEM and BET characterizations demonstrated that both common and mild combustion processes not only control the particle/crystal size but also improve the macroporous morphology and specific surface area. The superior CO_2 sorption properties of MC-0.4 were attributed to the smallest particle/crystal size, macroporous morphology, and largest specific surface area.

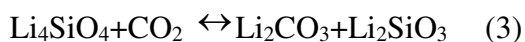
The DSC tests for MC-0.6 under 15 vol.% CO_2 from 100 to 800°C were performed to elucidate the eutectic phases generated during CO_2 dynamic sorption. As shown in Fig. 6, the heat flow graph slowly rose between 100 and $\sim 400^\circ\text{C}$ as demonstrated by a slow superficial-sorption in the TG curve. After $\sim 400^\circ\text{C}$, a sharp exothermic slope with a peak at $\sim 500^\circ\text{C}$ was evident due to fast-sorption of CO_2 which reacts

exothermically. Beyond $\sim 600\text{ }^{\circ}\text{C}$, an even stronger endothermic peak ($\sim 720\text{ }^{\circ}\text{C}$) becomes clearly evident in the DSC curves, which is associated with the desorption process. Similar exothermic/endothermic peaks were also observed by previous researchers [46]. Unexpectedly, between the exothermic peak and the endothermic peak, there was a weak endothermic peak, which appears to be related to the formation of the eutectic phases. The same DSC curve (green line) was also examined to confirm that the existence of a eutectic peak at $\sim 550\text{ }^{\circ}\text{C}$. Normally, such a eutectic peak is detected in alkali salts-doped Li_4SiO_4 . However, for the first time, we have verified the existence of eutectic phases for un-doped Li_4SiO_4 , which significantly promotes the diffusion process.

To further elucidate the features of this system and in particular identify the compositions of eutectic melt phases, a series of tests were performed using the MC-0.6 upon isothermal CO_2 at $580\text{ }^{\circ}\text{C}$ for 120 min under 15 vol.% CO_2 , considering that these eutectic phases formed during CO_2 sorption. First, as illustrated in Fig. 3b, after sorption, the main phases of Li_2SiO_3 or Li_2CO_3 were identified in the XRD patterns. A minor phase for Li_4SiO_4 was also observed, which is in agreement with the results of Fig. 1b. and suggested that most of the Li_4SiO_4 had reacted with CO_2 to form Li_2SiO_3 and Li_2CO_3 as proposed in equation (3) [47]. In the case of the SEM images of MC-0.6 after sorption (Fig. 4d), it showed a smooth and markedly sintered polyhedron covered by agglomerates of small nanoparticles ($\sim 100\text{ nm}$), with a framework of macropores. The EDX mapping results (Fig. 7) further confirm that these sintered polyhedron (Li_2CO_3), have most likely experienced a melt state, supporting the existence of eutectic

phases seen in DSC results. Such macroporous structures of nano-sized Li_2SiO_3 are extremely desirable for enhancing the CO_2 transportation to the interior of the agglomerates. Furthermore, macroporous and nano-sized Li_2SiO_3 is more convenient to react with Li_2CO_3 to recover Li_4SiO_4 than the case of SS (Fig. 1f). XPS analysis was also used to further study the distribution of eutectic melt phases. Si 2p, C 1s and Li 1s spectra of the MC-0.6 before and after CO_2 sorption were compared, as presented in Fig. 8. The binding energies of Si 2p for MC-0.6 (Fig. 8a) were ~ 100.7 eV, associated with the presence of a Li_4SiO_4 species [48]. After sorption, the peak area of spectra increased significantly, suggested that the atomic concentrations of Si became enriched on the surface, corresponding to the formation of Li_2SiO_3 , due to its higher molar ratio of Si/Li than Li_4SiO_4 . Moreover, the peak of the spectra shifted to higher binding energies, implying the presence of Li_2SiO_3 , as it has a higher binding energy than Li_4SiO_4 [48]. As illustrated in Fig. 8b, the C 1s component for the MC-0.6 before CO_2 sorption appeared at ~ 589.2 eV, corresponding to the species of carbonates [49] derived from Li_2CO_3 . The appearance of carbonates was due to trapping of CO_2 in the air, as reported previously [15]. After sorption, the peak area of carbonates should be greatly enlarged, but in this case remained almost constant suggesting that most of the generated Li_2CO_3 was not on the surface of particles. As shown in Fig. 8c, the Li 1s spectra of MC-0.6 exhibited a peak at 54.0 eV, which is related to the presence of a Li_xSiO_y phase [50]. After sorption, its maximum peak shifted to lower binding energies, which were associated with the formation of Li_2SiO_3 rather than Li_2CO_3 due to the higher binding energy (55.2-55.5 eV) for Li_2CO_3 [51]. The XPS analysis supported the

SEM results, and further suggested that Li_2SiO_3 was found on the surface whereas most of Li_2CO_3 was distributed inside the particles. It should be noted that an element concentration evolution as a function of the analysis depth will be conducted to further confirm this special structure.



3.4 Proposed CO_2 Sorption Mechanism

From the experimental evidence, nanoporous morphologies and induced molten shell model was proposed to explain the superior sorption for MC-0.6 as schematically illustrated in Fig. 9. Initially, based on isothermal experiments (Fig. 1d), when MC-0.6 was exposed to 15 vol.% CO_2 at low temperatures (200 and 500 °C) below the eutectic melting point ($\sim 550^\circ\text{C}$), the CO_2 molecules were assumed to be rapidly chemisorbed on the surface of the Li_4SiO_4 to generate a thin external layer. At this stage, as temperatures increased, the surface-sorption activity increased. Moreover, the XRD, SEM and BET characterizations further demonstrated the more favorable porous properties (such as nano-sized particle and large specific surface area) of MC-0.6. Kinetic analysis also supported the conclusion that surface sorption for MC-0.6 is less reliant on temperature, as its surface-sorption activity was higher than SS and CC (Fig. 1a).

After completion of the surface-sorption period, a bulk diffusion process started involving CO_2 diffusion and Li^+ and O_2 ionic diffusion, which becomes a barrier preventing the CO_2 from continuing to react with the remaining Li_4SiO_4 . Due to the solid layer of SS together with its extremely large and dense morphology as reported

by previous studies [15], a large diffusion barrier towards CO₂ occurs, results in the very low CO₂ uptake even at high temperature (i.e. 580 °C). By contrast, macroporous structures of nano-sized Li₂SiO₃ covered on the molten layer of Li₂CO₃ were confirmed by XRD, SEM and XPS characterizations. These macroporous structures accelerate the transportation of CO₂ into the centre of the particles. At the same time, both Li⁺ and O²⁻ are able to diffuse through a molten layer toward CO₂ with much less resistance. Therefore, the kinetics of surface-sorption and diffusion are both faster for MC-0.6 (Table 1).

Most previous models [7] proposed that the Li₂CO₃ covered on the layer of Li₂SiO₃. Here, we suggested a new structure (macroporous nano-sized Li₂SiO₃ covering on the melt layer of Li₂CO₃). Both models are combined to be a complete CO₂ sorption mechanism of pure Li₄SiO₄ surface.

4. Conclusions

Through a simple and cost-effective glucose-based mild combustion method, we have successfully prepared a highly efficient pure Li₄SiO₄ capable of capturing CO₂. At the optimized molar ratio of glucose:LiNO₃ with 0.6:1, MC-0.6 reached a maximum sorption capacity (~35.0 wt.%) at 580 °C under 15 vol.% CO₂, which is the largest CO₂ sorption capacity for pure Li₄SiO₄ under 15 vol.% CO₂ reported in the literature to date. Moreover, a high capacity was maintained over 10 sorption/desorption cycles. MC-0.6 presented a highly porous nano-agglomerate (50-100 nm) morphology, allowing a rapid surface-sorption of CO₂. Also, for the first time, the existence of a new structure (macroporous nano-sized Li₂SiO₃ covering on the melt layer of Li₂CO₃) was identified,

which noticeably facilitated the transportation of CO_2 and decreased the Li^+ and O^{2-} ionic diffusion resistance through the molten layer toward more CO_2 . Thus, both surface-sorption and diffusion kinetics impedance by low CO_2 concentrations were greatly reduced, demonstrating that the slow kinetics of Li_4SiO_4 at a low CO_2 concentration can be eliminated by morphological control instead of the traditional doping approach.

Acknowledgement

This work was supported by financial supports from the Fundamental Research Funds for the Central Universities (2018XKQYMS13).

References

- [1] W. Cai, A. Santoso, G. Wang, S.W. Yeh, S.I. An, K.M. Cobb, M. Collins, E. Guilyardi, F.F. Jin, J.S. Kug, M. Lengaigne, M.J. McPhaden, K. Takahashi, A. Timmermann, G. Vecchi, M. Watanabe, L. Wu, ENSO and greenhouse warming, *Nat. Clim. Change* 5 (2015) 849-859.
- [2] S. Brune, S.E. Williams, R.D. Müller, Potential links between continental rifting, CO_2 degassing and climate change through time, *Nat. Geosci.* 10 (2017) 941-946.
- [3] J. Rissman, C. Bataille, E. Masanet, N. Aden, W.R. Morrow, N. Zhou, N. Elliott, R. Dell, N. Heeren, B. Huckestein, J. Cresko, S.A. Miller, J. Roy, P. Fennell, B. Cremmins, T. Koch Blank, D. Hone, E.D. Williams, S. de la Rue du Can, B. Sisson, M. Williams, J. Katzenberger, D. Burtraw, G. Sethi, H. Ping, D. Danielson, H. Lu, T. Lorber, J. Dinkel, J. Helseth, Technologies and policies to decarbonize global industry: Review and assessment of mitigation drivers through 2070, *Appl. Energy* 266 (2020) 114848.
- [4] X. Kou, C. Li, Y. Zhao, S. Wang, X. Ma, CO_2 sorbents derived from capsule-connected Ca-Al hydrotalcite-like via low-saturated coprecipitation, *Fuel Process. Technol.* 177 (2018) 210-218.
- [5] S. Jin, K. Ho, C.H. Lee, Facile synthesis of hierarchically porous MgO sorbent doped with CaCO_3 for fast CO_2 capture in rapid intermediate temperature swing sorption, *Chem. Eng. J.* 334 (2018) 1605-1613.
- [6] A.T. Vu, Y. Park, P.R. Jeon, C.H. Lee, Mesoporous MgO sorbent promoted with KNO_3 for CO_2 capture at intermediate temperatures, *Chem. Eng. J.* 258 (2014) 254-264.
- [7] Y. Zhang, Y. Gao, H. Pfeiffer, B. Louis, L. Sun, D. O'Hare, Q. Wang, Recent advances in lithium containing ceramic based sorbents for high-temperature CO_2 capture, *J. Mater. Chem. A* 7 (2019) 7962-8005.
- [8] D. He, Z. Ou, C. Qin, T. Deng, J. Yin, G. Pu, Understanding the catalytic acceleration effect of steam on CaCO_3 decomposition by density function theory, *Chem. Eng. J.* 379 (2020) 122348.
- [9] H. Wang, Z. Li, N. Cai, Multiscale model for steam enhancement effect on the carbonation of CaO particle, *Chem. Eng. J.* 394 (2020) 124892.

- [10] W. Zhang, Y. Li, B. Li, Y. Wang, Y. Qian, Z. Wang, Simultaneous NO/CO₂ removal by Cu-modified biochar/CaO in carbonation step of calcium looping process, *Chem. Eng. J.* 392 (2020) 123659.
- [11] M. Bui, C.S. Adjiman, A. Bardow, E.J. Anthony, A. Boston, S. Brown, P.S. Fennell, S. Fuss, A. Galindo, L.A. Hackett, J.P. Hallett, H.J. Herzog, G. Jackson, J. Kemper, S. Krevor, G.C. Maitland, M. Matuszewski, I.S. Metcalfe, C. Petit, G. Puxty, J. Reimer, D.M. Reiner, E.S. Rubin, S.A. Scott, N. Shah, B. Smit, J.P.M. Trusler, P. Webley, J. Wilcox, N. Mac Dowell, Carbon capture and storage (CCS): the way forward, *Energy Environ. Sci.* 11 (2018) 1062-1176.
- [12] G. Ji, J.G. Yao, P.T. Clough, J.C.D. da Costa, E.J. Anthony, P.S. Fennell, W. Wang, M. Zhao, Enhanced hydrogen production from thermochemical processes, *Energy Environ. Sci.* 11 (2018) 2647-2672.
- [13] L.C. Buelens, H. Poelman, G.B. Marin, V.V. Galvita, 110th Anniversary: Carbon Dioxide and Chemical Looping: Current Research Trends, *Ind. Eng. Chem. Res.* 58 (2019) 16235-16257.
- [14] L.C. Buelens, V.V. Galvita, H. Poelman, C. Detavernier, G.B. Marin, Super-dry reforming of methane intensifies CO₂ utilization via Le Chatelier's principle, *Science* 354 (2016) 449-452.
- [15] Y. Hu, W. Liu, Y. Yang, M. Qu, H. Li, CO₂ capture by Li₄SiO₄ sorbents and their applications: Current developments and new trends, *Chem. Eng. J.* 359 (2019) 604-625.
- [16] M. Kato, K. Nakagawa, New Series of Lithium Containing Complex Oxides, Lithium Silicates, for Application as a High Temperature CO₂ Absorbent, *J. Ceram. Soc. Jpn.* 109 (2001) 911-914.
- [17] M.J. Venegas, E. Fregoso-Israel, R. Escamilla, H. Pfeiffer, Kinetic and Reaction Mechanism of CO₂ Sorption on Li₄SiO₄: Study of the Particle Size Effect, *Ind. Eng. Chem. Res.* 46 (2007) 2407-2412.
- [18] Z. Yin, K. Wang, P. Zhao, X. Tang, Enhanced CO₂ Chemisorption Properties of Li₄SiO₄, Using a Water Hydration–Calcination Technique, *Ind. Eng. Chem. Res.* 55 (2016) 1142-1146.
- [19] P.V. Subha, B.N. Nair, P. Hareesh, A.P. Mohamed, T. Yamaguchi, K.G.K. Warriar, U.S. Hareesh, Enhanced CO₂ absorption kinetics in lithium silicate platelets synthesized by a sol-gel approach, *J. Mater. Chem. A* 2 (2014) 12792-12798.
- [20] L. Ma, C. Qin, S. Pi, H. Cui, Fabrication of efficient and stable Li₄SiO₄-based sorbent pellets via extrusion-spheronization for cyclic CO₂ capture, *Chem. Eng. J.* 379 (2020) 122385.
- [21] S. Shan, S. Li, Q. Jia, L. Jiang, Y. Wang, J. Peng, Impregnation Precipitation Preparation and Kinetic Analysis of Li₄SiO₄-Based Sorbents with Fast CO₂ Adsorption Rate, *Ind. Eng. Chem. Res.* 52 (2013) 6941-6945.
- [22] M.T. Izquierdo, A. Turan, S. García, M.M. Maroto-Valer, Optimization of Li₄SiO₄ synthesis conditions by a solid state method for maximum CO₂ capture at high temperature, *J. Mater. Chem. A* 6 (2018) 3249-3257.
- [23] A. Nambo, J. He, T.Q. Nguyen, V. Atla, T. Druffel, M. Sunkara, Ultrafast Carbon Dioxide Sorption Kinetics Using Lithium Silicate Nanowires, *Nano Lett.* 17 (2017) 3327-3333.
- [24] G.J. Rao, R. Mazumder, S. Bhattacharyya, P. Chaudhuri, Synthesis, CO₂ absorption property and densification of Li₄SiO₄ powder by glycine-nitrate solution combustion method and its comparison with solid state method, *J. Alloys Compd.* 725 (2017) 461-471.
- [25] Y. Hu, W. Liu, Y. Yang, X. Tong, Q. Chen, Z. Zhou, Synthesis of highly efficient, structurally improved Li₄SiO₄ sorbents for high-temperature CO₂ capture, *Ceram. Int.* 44 (2018) 16668-16677.
- [26] M. Zhao, H. Fan, F. Yan, Y. Song, X. He, M.Z. Memon, S.K. Bhatia, G. Ji, Kinetic analysis for cyclic CO₂ capture using lithium orthosilicate sorbents derived from different silicon precursors, *Dalton Trans.* 47 (2018) 9038-9050.
- [27] Q. Zhang, D.Y. Han, Y. Liu, Q. Ye, Z.B. Zhu, Analysis of CO₂ Sorption/Desorption Kinetic

Behaviors and Reaction Mechanisms on Li_4SiO_4 , *AIChE J.* 59 (2013) 901-911.

- [28] M. Seggiani, M. Puccini, S. Vitolo, High-temperature and low concentration CO_2 sorption on Li_4SiO_4 based sorbents: Study of the used silica and doping method effects, *Int. J. Greenhouse Gas Control* 5 (2011) 741-748.
- [29] J. Ortiz-Landeros, I.C. Romero-Ibarra, C. Gómez-Yáñez, E. Lima, H. Pfeiffer, $\text{Li}_{4+x}(\text{Si}_{1-x}\text{Al}_x)\text{O}_4$ Solid Solution Mechanosynthesis and Kinetic Analysis of the CO_2 Chemisorption Process, *J. Phys. Chem. C* 117 (2013) 6303-6311.
- [30] C. Gauer, W. Heschel, Doped lithium orthosilicate for absorption of carbon dioxide, *J. Mater. Sci.* 41 (2006) 2405-2409.
- [31] M. Xiang, Y. Zhang, M. Hong, S. Liu, Y. Zhang, H. Liu, C. Gu, CO_2 absorption properties of Ti- and Na-doped porous Li_4SiO_4 prepared by a sol-gel process, *J. Mater. Sci.* 50 (2015) 4698-4706.
- [32] X. Chen, Z. Xiong, Y. Qin, B. Gong, C. Tian, Y. Zhao, J. Zhang, C. Zheng, High-temperature CO_2 sorption by Ca-doped Li_4SiO_4 sorbents, *Int. J. Hydrogen Energy* 41 (2016) 13077-13085.
- [33] P.V. Subha, B.N. Nair, P. Hareesh, A.P. Mohamed, T. Yamaguchi, K.G.K. Warriar, U.S. Hareesh, CO_2 Absorption Studies on Mixed Alkali Orthosilicates Containing Rare-Earth Second-Phase Additives, *J. Phys. Chem. C* 119 (2015) 5319-5326.
- [34] M. Seggiani, M. Puccini, S. Vitolo, Alkali promoted lithium orthosilicate for CO_2 capture at high temperature and low concentration, *Int. J. Greenhouse Gas Control* 17 (2013) 25-31.
- [35] V.L. Meja-Trejo, E. Fregoso-Israel, H. Pfeiffer, Textural, Structural, and CO_2 Chemisorption Effects Produced on the Lithium Orthosilicate by Its Doping with Sodium ($\text{Li}_{4-x}\text{Na}_x\text{SiO}_4$), *Chem. Mater.* 20 (2008) 7171-7176.
- [36] X. Yang, W. Liu, J. Sun, Y. Hu, W. Wang, H. Chen, Y. Zhang, X. Li, M. Xu, Alkali-Doped Lithium Orthosilicate Sorbents for Carbon Dioxide Capture, *ChemSusChem* 9 (2016) 2480-2487.
- [37] H. Cui, X. Li, H. Chen, X. Gu, Z. Cheng, Z. Zhou, Sol-gel derived, Na/K-doped Li_4SiO_4 -based CO_2 sorbents with fast kinetics at high temperature, *Chem. Eng. J.* 382 (2020) 122807.
- [38] K. Wang, Z.Y. Zhou, P.F. Zhao, Z.G. Yin, Z. Su, J. Sun, Molten sodium-fluoride-promoted high-performance Li_4SiO_4 -based CO_2 sorbents at low CO_2 concentrations, *Appl. Energy* 204 (2017) 403-412.
- [39] K. Wang, W. Li, Z. Yin, Z. Zhou, P. Zhao, High-Capacity Li_4SiO_4 -Based CO_2 Sorbents via a Facile Hydration-NaCl Doping Technique, *Energy & Fuels* 31 (2017) 6257-6265.
- [40] P.V. Subha, B.N. Nair, A.P. Mohamed, G.M. Anilkumar, K.G.K. Warriar, T. Yamaguchi, U.S. Hareesh, Morphologically and compositionally tuned lithium silicate nanorods as high-performance carbon dioxide sorbents, *J. Mater. Chem. A* 4 (2016) 16928-16935.
- [41] H. Li, M. Qu, Y. Hu, Preparation of spherical Li_4SiO_4 pellets by novel agar method for high-temperature CO_2 capture, *Chem. Eng. J.* 380 (2020) 122538.
- [42] X. Yang, W. Liu, J. Sun, Y. Hu, W. Wang, H. Chen, Y. Zhang, X. Li, M. Xu, Preparation of Novel Li_4SiO_4 Sorbents with Superior Performance at Low CO_2 Concentration, *ChemSusChem* 9 (2016) 1607-1613.
- [43] I.C. Romero-Ibarra, J. Ortiz-Landeros, H. Pfeiffer, Microstructural and CO_2 chemisorption analyses of Li_4SiO_4 : Effect of surface modification by the ball milling process, *Thermochim. Acta* 567 (2013) 118-124.
- [44] K. Wang, J. Hong, Z. Zhou, Z. Lin, P. Zhao, Development of Alkali Nitrate-Containing Li_4SiO_4 for High-Temperature CO_2 Capture, *Energy Technol.* 7 (2019) 325-332.
- [45] K. Wang, Y. Zhao, P.T. Clough, P. Zhao, E.J. Anthony, Sorption of CO_2 on NaBr co-doped Li_4SiO_4 ceramics: Structural and kinetic analysis, *Fuel Process. Technol.* 195 (2019) 106143.

- [46] M. Niu, X. Li, J. Ouyang, H. Yang, Lithium orthosilicate with halloysite as silicon source for high temperature CO₂ capture, *RSC Adv.* 6 (2016) 44106-44112.
- [47] K. Nakagawa, T. Ohashi, A Novel Method of CO₂ Capture from High Temperature Gases, *J. Electrochem. Soc.* 145 (1998) 1344-1346.
- [48] B. Philippe, R. Dedryvere, M. Gorgoi, H. Rensmo, D. Gonbeau, K. Edstrom, Role of the LiPF₆ Salt for the Long-Term Stability of Silicon Electrodes in Li-Ion Batteries - A Photoelectron Spectroscopy Study, *Chem. Mater.* 25 (2013) 394-404.
- [49] B.T. Young, D.R. Heskett, C.C. Nguyen, M. Nie, J.C. Woicik, B.L. Lucht, Hard X-ray Photoelectron Spectroscopy (HAXPES) Investigation of the Silicon Solid Electrolyte Interphase (SEI) in Lithium-Ion Batteries, *ACS Appl Mater Interfaces* 7 (2015) 20004-20011.
- [50] E. Radvanyi, E. De Vito, W. Porcher, S. Jouanneau Si Larbi, An XPS/AES comparative study of the surface behaviour of nano-silicon anodes for Li-ion batteries, *J. Anal. At. Spectrom.* 29 (2014) 1120-1131.
- [51] D. Aurbach, I. Weissman, A. Schechter, H. Cohen, X-ray Photoelectron Spectroscopy Studies of Lithium Surfaces Prepared in Several Important Electrolyte Solutions. A Comparison with Previous Studies by Fourier Transform Infrared Spectroscopy, *Langmuir* 12 (1996) 3991-4007.

Table 1. Kinetic parameters obtained from the isothermal profiles.

Samples	T[°C]	k_1	k_2	A	B	C	R
MC-0.6	500	1.51×10^{-1}	1.03×10^{-2}	-36.44	-21.55	134.24	0.999
	540	2.26×10^{-1}	2.83×10^{-2}	-26.11	-3.57	130.48	0.999
	580	3.25×10^{-1}	7.20×10^{-2}	-47.42	-1.99	134.30	0.999
CC	580	1.57×10^{-1}	1.10×10^{-2}	-30.29	-1.42	128.92	0.999
SS	580	1.05×10^{-1}	9.01×10^{-3}	-4.69	-9.89	116.56	0.999

Table 2. N₂ adsorption/desorption results of samples

Samples	Surface area (m ² /g)	Pore volume (cc/g)	Average pore diameter (nm)
SS	0.4	0.003	17
CC	13.6	0.026	2
MC-0.6	17.4	0.041	5

Figure captions:

Fig. 1. CO₂ uptake characteristics of prepared samples. (a) Dynamic thermogravimetric curves between 100 and 900 °C in a 15% CO₂ flux; (b) Isothermal curves of three samples derived from different preparation methods at 580 °C; (c) Dynamic sorption curves of three samples with different amount of glucose; (d) Isothermal curves of the MC-0.6 at different temperatures; (e) Cyclic performance of the MC-0.6 sample during 10 cycles of sorption/desorption; (f) Isothermal desorption curve at 700 °C in a pure N₂ flux.

Fig. 2. Eyring's plots for the rate constants of surface-sorption (k_1) and bulk diffusion (k_2) for MC-0.6.

Fig. 3. XRD patterns of the three sample (a) Fresh samples; (b) MC-0.6 after sorption.

Fig. 4. SEM images of different samples: (a) SS, (b) CC, (c) MC-0.6 and (d) MC-0.6 after sorption.

Fig. 5. N₂ adsorption/desorption isotherms of three sorbents; (b) BJH pore size distribution of MC-0.6.

Fig. 6. Dynamic DSC analysis of MC-0.6 between 100 and 800 °C in a 15% CO₂ flux.

Fig. 7. SEM micrograph and chemical mapping of MC-0.6 after sorption. (a) SEM image; (b) Si mapping; (c) C mapping; (d) O mapping.

Fig. 8. XPS spectra of MC-0.6 before and after sorption. (a) Si 2p spectra; (b) C 1s spectra; (c) Li 1s spectra.

Fig. 9. Schematic illustration of double-shell mechanism occurred in MC-0.6 where transparent pores representing macropores.

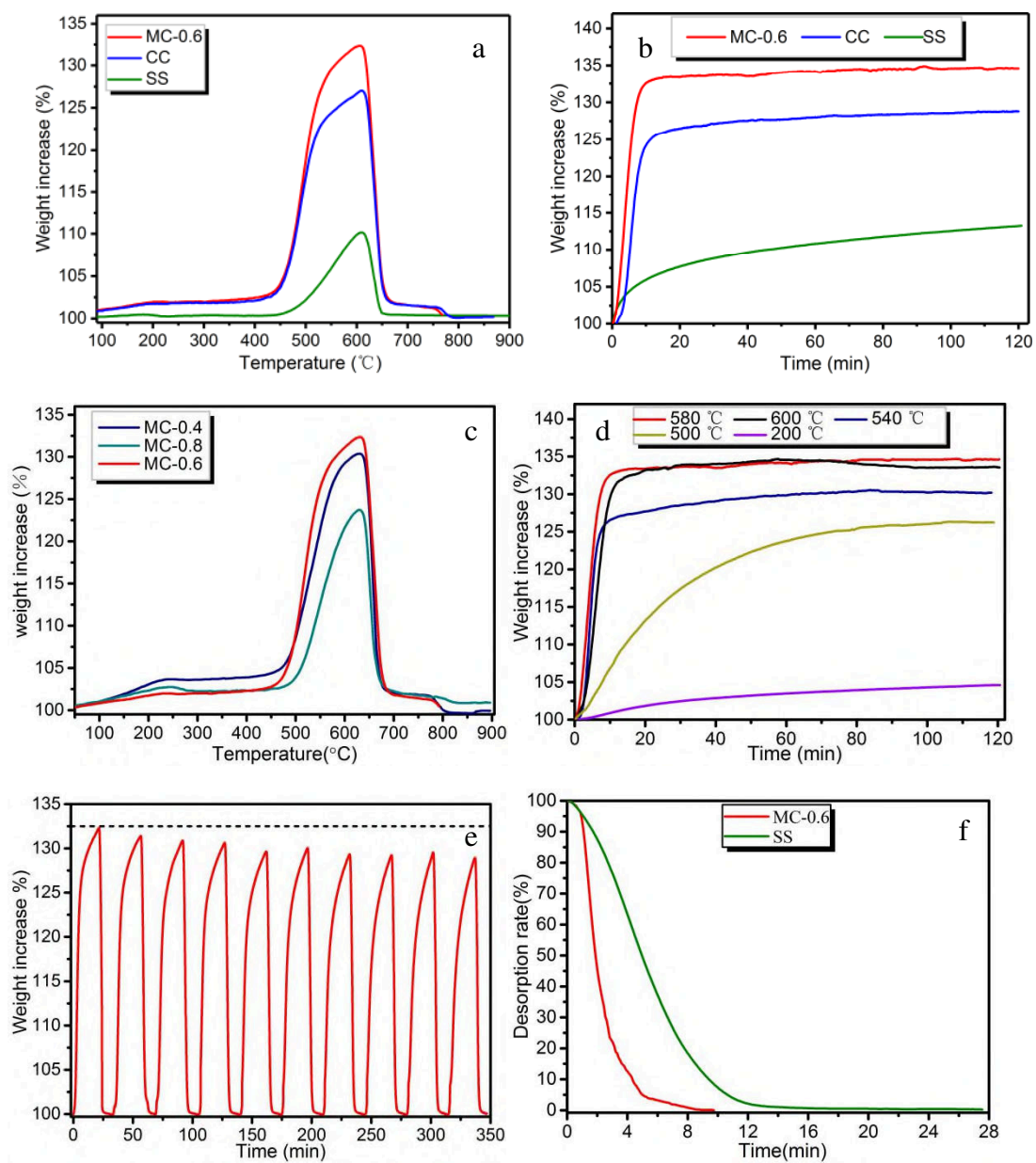


Fig. 1.

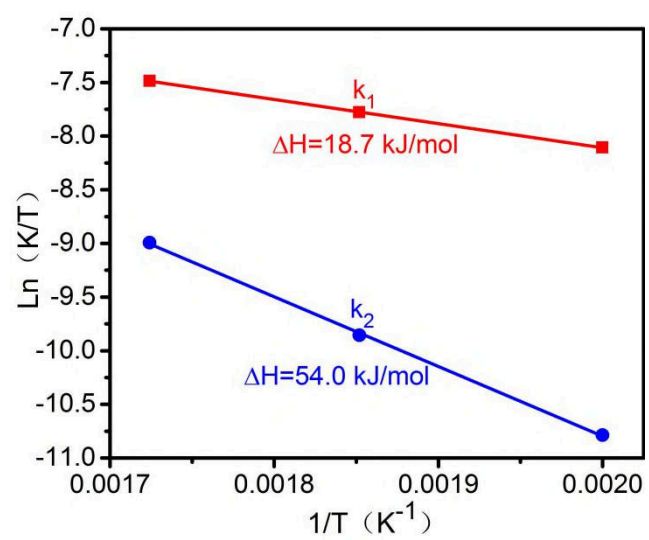


Fig. 2.

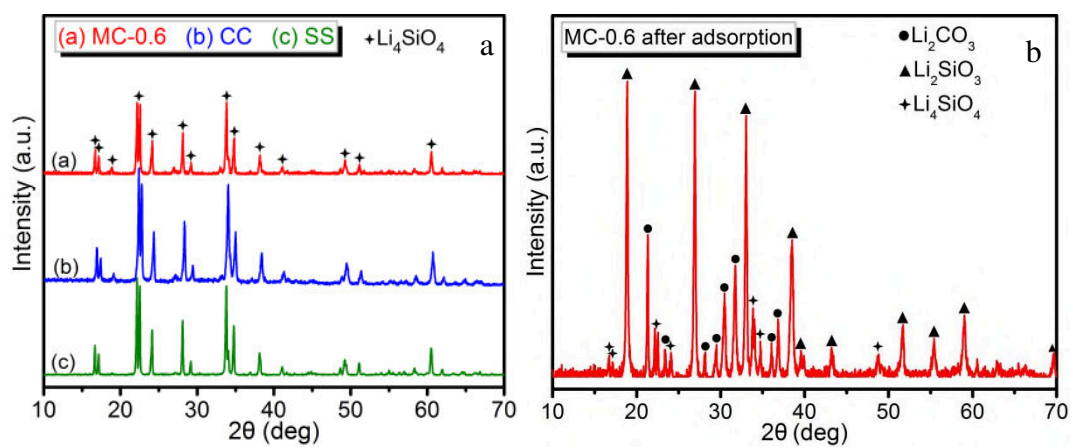


Fig. 3.

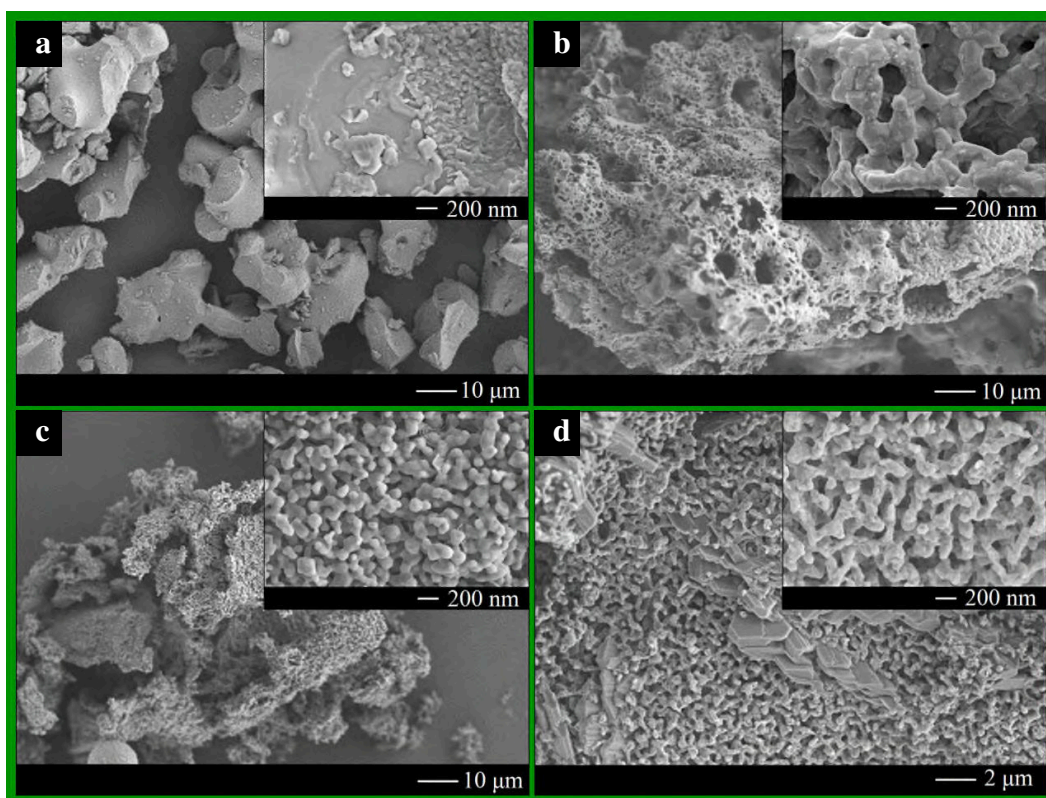


Fig. 4.

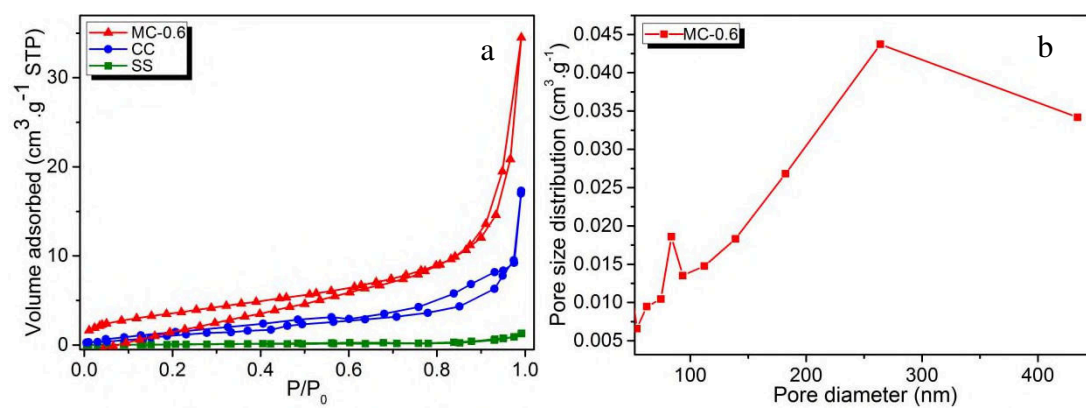


Fig. 5.

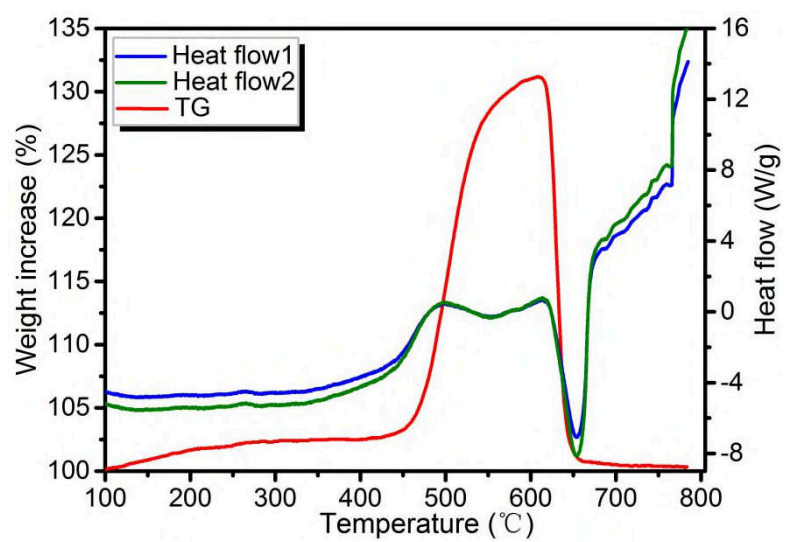


Fig. 6.

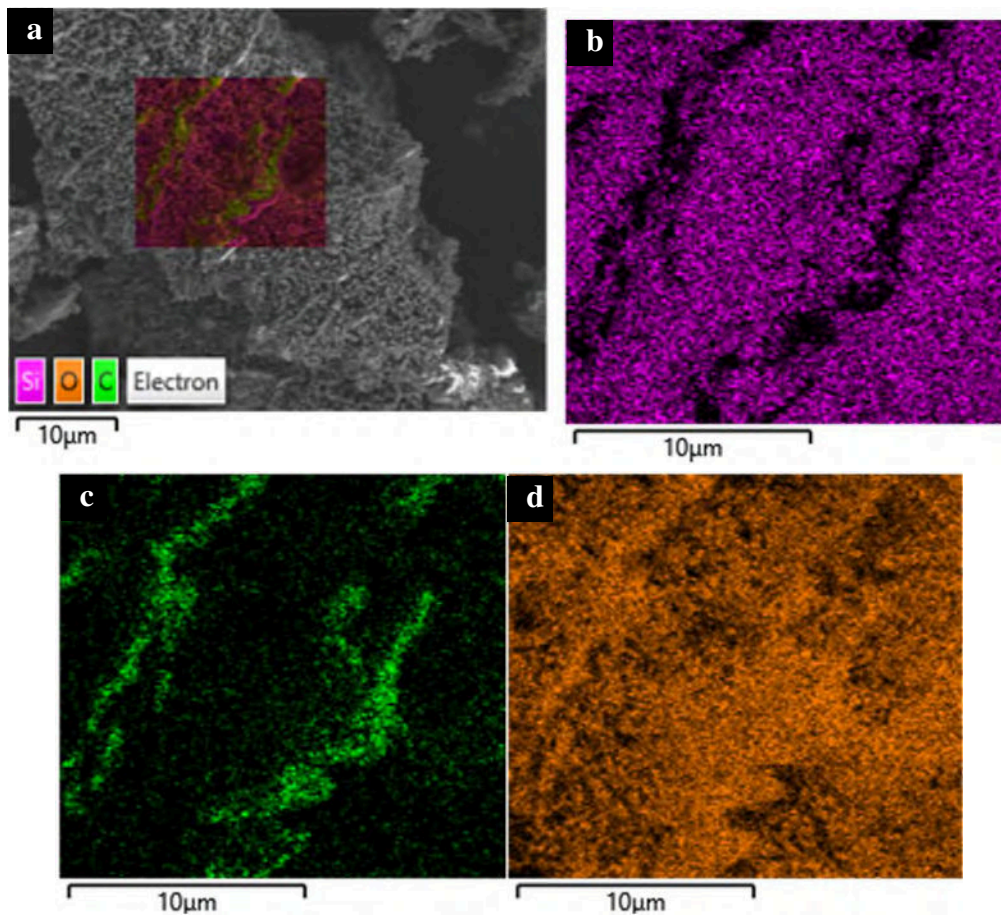


Fig. 7.

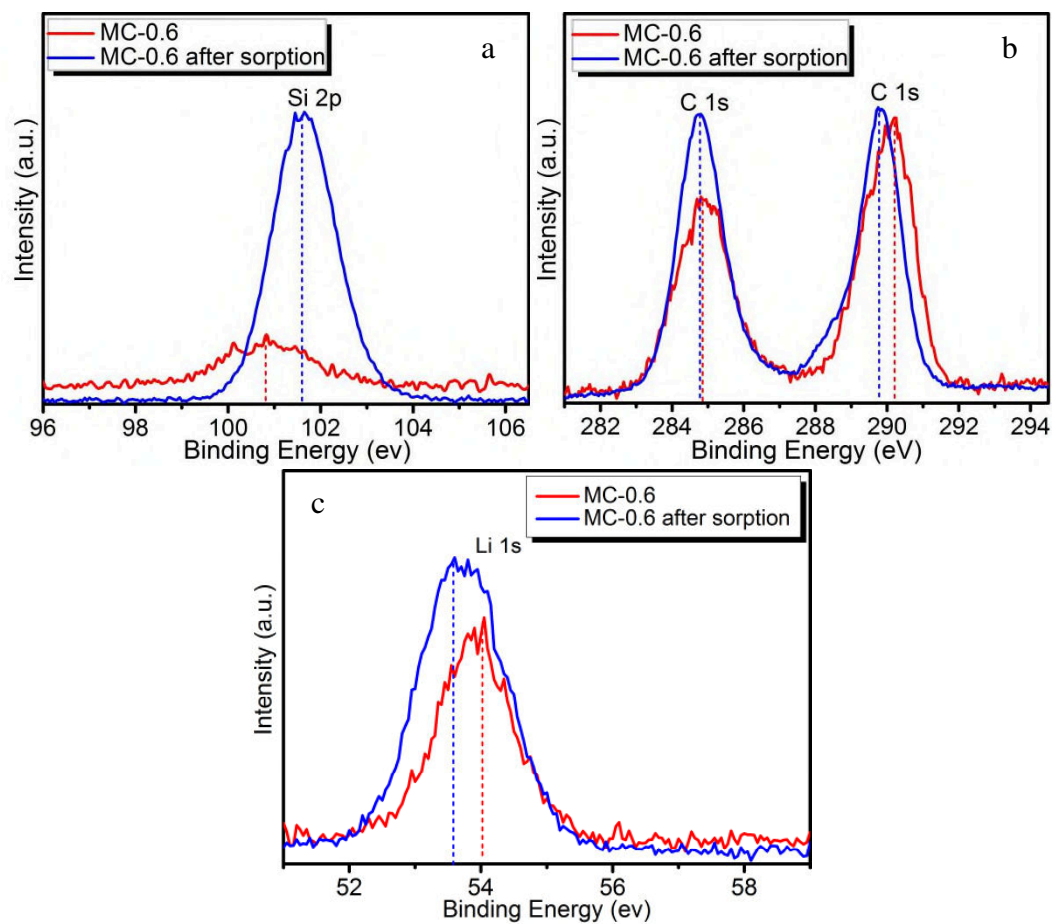


Fig. 8.

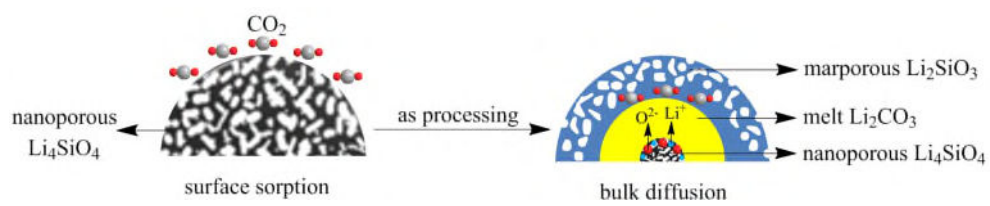


Fig. 9.

Molten shell-activated, high-performance, un-doped Li₄SiO₄ for high-temperature CO₂ capture at low CO₂ concentrations

Wang, Ke

2020-10-16

Attribution-NonCommercial-NoDerivatives 4.0 International

Wang K, Gu F, Clough PT, et al., (2020) Molten shell-activated, high-performance, un-doped Li₄SiO₄ for high-temperature CO₂ capture at low CO₂ concentrations. Chemical Engineering Journal, Volume 408, March 2021, Article number 127353

<https://doi.org/10.1016/j.cej.2020.127353>

Downloaded from CERES Research Repository, Cranfield University